ELSEVIER

Journal of Electroanalytical Chemistry 444 (1998) 155–167

JOURNAL OF ELECTROANALYTICAL CHEMISTRY

Calorimetry close to the boiling temperature of the D_2O/Pd electrolytic system

G. Mengoli [a,*], M. Bernardini [a], C. Manduchi [b], G. Zannoni [b]

[a] *CNR IPELP, Corso Stati Uniti 4, 35127 Padova, Italy*
[b] *Dipartimento di Fisica dell'Università di Padova, via Marzolo 8, 35131 Padova, Italy*

Received 26 January 1996; received in revised form 31 May 1996

Abstract

The electrolytic insertion of deuterium into Pd at 95°C was investigated by a simple calorimetric technique. This involved continuous feeding of heating power to the electrolytic cell to maintain it isothermal with an external thermostatic bath: any extraneous thermal phenomenon taking place inside the cell is directly determined by the lack of balance of the original heating power input. It was thus found that Pd loading by deuterium is always paralleled by excess power generation, which largely exceeds the electrolytic power input. After prolonged electrolysis the loaded electrodes were found to continue heat generation in open circuit (o.c.) conditions. The reproducibility of the thermal phenomenon allowed its dependence on several experimental parameters to be investigated.

Keywords: Calorimetry; Temperature; D_2O/Pd electrolytic system

1. Introduction

Since the announcement of 'Cold Fusion' in 1989 [1,2] a great deal of investigation has been focused on the calorimetry of D_2O electrolysis at the Pd cathode.

In attempts to reproduce the anomalous heat effects reported by Fleischmann et al. [1,3], their original protocol has generally been followed: calorimetric data are gathered from a Dewar type electrolytic cell immersed in a bath thermostated at about room temperature (30°C); LiOD is the preferred electrolyte; Pd cathodes are rod-shaped; the electrolyses are carried out at low and then at high current densities. The target is to force into the Pd lattice a large concentration of deuterium which is considered the necessary condition for inducing anomalous heat effects.

Indeed, much controversy has arisen out of this approach, as excess enthalpy generation has been observed by some researchers [4–7], but a number of investigations were totally negative [4–7]. Although the many positive findings cannot be ignored, there is a persistent reluctance by the scientific community to accept a phenomenon which appears to be so elusive and sporadic.

In recent years the insertion of deuterium into Pd and the correlated anomalous heat generation have also been achieved by experimental environments different from the original one. Thus, in 1991, Liaw et al. [8] reported the use of an electrochemical cell, Pd|eutectic LiCl + KCl saturated with LiD|Al, working at 350°C. In this case excess heat was correlated with deuterium loaded into a Pd anode via the oxidation of LiD. The reproducibility was low, but the extent of the thermal phenomenon (absolute excess power = 10–25 W; excess power gain 600–1500%) was such as to exclude measurement errors or artefacts.

In 1992, new results for glow discharge in deuterium calorimetry were presented by Karabut et al. [9]. The discharge was performed at a Pd cathode well above

* Corresponding author. Istituto di Polarografia, CNR IPELP, Corso Stati Uniti 4, 35020 Padova, Italy. Fax: +39.49 8295853

0022-0728/98/$19.00
PII S0022-0728(97)00634-7

100°C and heat output five times exceeding the input electric power was observed. According to the authors "excess heat power was registered in most experiments" [10].

In 1993, Fleischmann and Pons [11] published the calorimetry of Pd-D_2O cells electrolytically driven to boiling point with total D_2O evaporation. Although the precision of the calorimetric results thus obtained was questioned [12], one unquestionable item of data did emerge: the Pd cathode remained hot ($t > 100$°C) for hours in the dried cell, which was no longer receiving electric power.

The environments of the above experiments [8–11] were such that high deuterium loading into the Pd lattice could hardly be achieved. Therefore, the trigger for the anomalous heat effects was very likely the use of temperature conditions well above room temperature: this fits with the observation of "positive feedback between the increase of temperature and the rate of generation of excess enthalpy" [11].

The present investigation started from the above considerations: this paper reports the calorimetric results obtained during D_2O electrolysis on Pd at an electrolyte temperature close to boiling.

2. Experimental

2.1. Materials

Pd of 99.9% purity came from two sources. One was a Russian company through Franco Suisse (Padova) and was shaped into sheets 0.02 and 0.05 cm thick: the metal was cold worked and the sheets were annealed at 800°C in Ar. The other was from Johnson Matthey through Metalli Preziosi (Milano) and was shaped as a rod of $\emptyset = 0.4$ cm. Before use, the Pd samples were washed with acetone, rinsed with H_2O and dipped for 20–30 min in 5 M HCl.

Ni wire of 99.5% purity was supplied by Carlo Erba (Milano); before use, the metal was etched in 1 M HCl (10 min), dipped for 1 day in hot 0.6 M K_2CO_3 and then left to dry in air to grow a coherent oxide layer.

D_2O at 99.8% isotopic purity came from Riedel-de Haën through Behring (Milano).

K_2CO_3 was reagent grade from Carlo Erba (Milano): this alkaline electrolyte was preferred to pure alkaline hydroxides because of its lower reactivity towards the glass components of the electrochemical cell.

N_2, D_2 and H_2 were high-purity gases supplied by S.I.O. (Padova). The cell and its glass components were made of Pyrex.

2.2. Apparatus

The experimental assembly used for obtaining calorimetric data from the electrolytic runs is shown in Fig. 1. It basically consists of: (1) a thermostated silicon oil bath; (2) a Dewar-type electrolytic cell equipped with a refrigerating column; (3) a gas line conveying a continuous stream of bubbles through the electrolyte.

The characteristics of each component are as follows.

(1) The silicon oil bath was kept temperature-stable at ± 0.01°C by an F3 Haake thermostat.

(2) The double-jacket glass cell had internal dimensions $\emptyset = 4$ cm and $h = 17$ cm, with useful capacity ≈ 110 cm^3 (it was generally charged with 90–100 ml of electrolytic solution). A glass joint at the side connected the cell with the refrigerating column. The top seal was a Teflon lid ($h = 5$ cm) supporting cathode, anode, heater, thermometer and glass pipe bubbler.

(3) The cathode was a Pd strip (or rod) tightened to a Pt wire which was fixed with Araldite epoxy resin inside a Pyrex tube to avoid any contact with either the electrolyte or the gas in the cell. Pd sheet electrodes were pressure bonded to Pt wire, whereas the Pd rod was connected by welding.

(4) The anode was a cylindrical coil (of diameter 3.7 cm) of Ni wire ($\emptyset = 0.1$ cm, $l = 130$ cm) which surrounded the cathode. External electrical connection was achieved by running the end of the Ni wire through a Pyrex tube sealed with epoxy resin up through the electrolyte and through the Teflon lid.

Cathode and anode were connected to a Model 553 Amel galvanostat, the potential difference applied being monitored by a Keithley 175A multimeter.

(5) The heater was a vertically standing device, constructed by coiling a nickel-chrome wire ($\emptyset = 0.03$ cm, $l = 90$ cm) onto a glass mesh support and then forcing it into a thin-walled Pyrex tube: this device was immersed into the cell to the bottom, the upper part of the resistive element being ≈ 5 cm below the electrolyte level.

The heater was fed, through Cu wire connections, by a Model 553 Amel galvanostat supplying dc current stabilised at ± 1%: applied voltage was monitored by a Keithley 175A multimeter.

(6) The thermometer was a Pt100 thermoresistance (length of the resistive element, 1.5 cm) sampled continuously by a Wheatstone bridge manufactured by Thermo Engineering (Cremona). The system was fed by a high-stability Model 401 Ortec 24 V power generator, and temperature was displayed as electric current by a Keithley 175A multimeter.

(7) The gas line comprised a compressed gas cylinder with valves controlling gas flow-rate. The presaturator was filled with D_2O. The glass pipe bubbler (placed out of the cell axis, cf. Fig. 1) was joined at less than 1 cm from the cell bottom, whereby the gas stream was

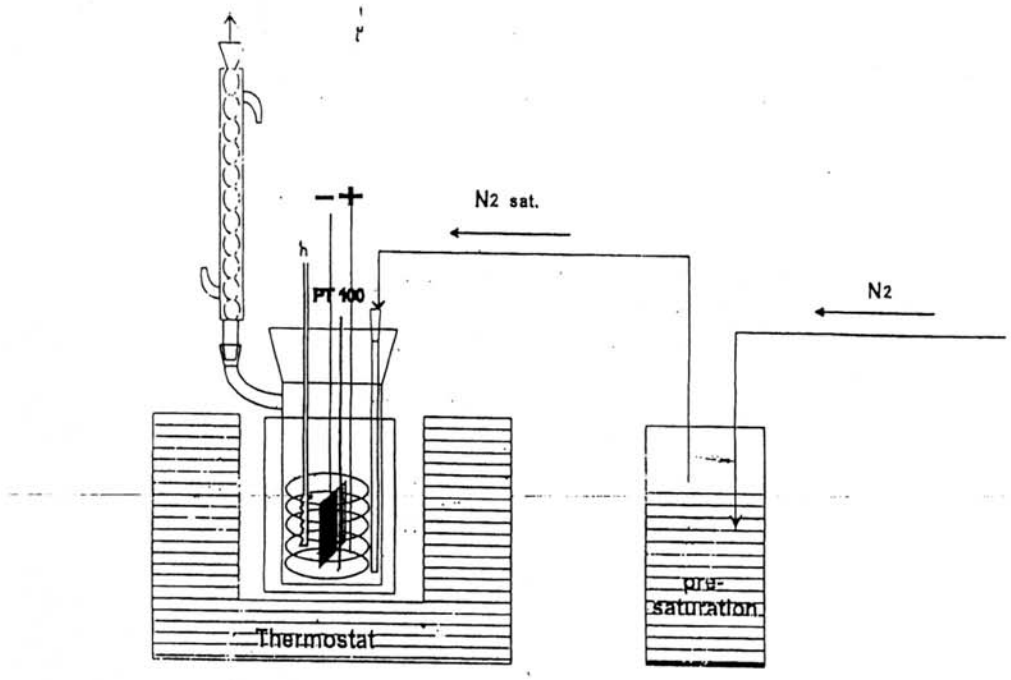

Fig. 1. Calorimetric system.

emitted and the bubbles were statistically distributed everywhere across the solution. The gas exited through the refrigerating column to an external bubbler containing paraffin which insulated the system from the atmosphere.

The gas flow, adjusted by the valves, was measured by counting the bubbles flowing in 1 min through the presaturator, this rate being standardised in ml min^{-1} by a flowmeter.

(8) The column was refrigerated by a controlled stream of H_2O using either tap water or deep drill water (the temperature of the latter was steady at 18°C). As shown in Fig. 1, the column was deliberately positioned outside the cell axis, condensed vapour thus reached the electrolyte after pre-heating across the lateral joint: the thermometric noise otherwise caused by cold drops falling directly into the cell was thus avoided.

2.3. Procedure

2.3.1. Characteristics of calorimeter

When the temperature of the oil bath was fixed at 95.00 ± 0.01°C (the selected working temperature), the temperature attained in the electrolyte was several degrees lower owing to cell heat loss. Some loss occurred through the lid and the part of the cell emerging from the bath: other losses were due to the large D_2O evaporation, vapour cooling in the column and D_2O reflux into the cell. When a gas stream, typically N_2, was bubbling through the solution, the heat loss rate due to gas heating from room temperature to 95°C was negligible (≈ 4 mW for the flow-rate usually adopted) but the heat loss due to increased D_2O evaporation was considerable.

As a consequence, gas flow (and its control) is very important, not only in stirring the electrolyte and granting uniform temperature distribution, but also in that it controls the heat loss characteristics of the cell. A high flow-rate gives high stirring but decreases the cell constant (in °C W^{-1}) and thus the sensitivity of the calorimeter: the opposite happens with a slow flow-rate. A flow-rate of 62 ± 1 bubbles per min, or 2.7 ml min^{-1}, was chosen as a compromise and this rate was then steadily maintained in all experiments.

2.3.2. Calibration

Once bath temperature and gas flow-rate had been fixed, to make the electrolyte isothermal with the oil bath, additional power had to be fed to the cell by the heater. Isothermal conditions were kept steady by constant heating power: changes in electrolyte temperature in time were well within 0.1°C, as variations of 1°C in the room were reflected by not more than 0.02–0.03°C in the electrolyte.

Under steady-state conditions the electrolyte receives heat, through lateral walls and the bottom, by the thermostat as well as internally by the heater, whereas heat is lost at the electrolyte surface: even under stirring

some temperature gradient must be established, the extent of which was investigated as follows. The Pt100, fitted on the lid ≈2.5 cm from the heater, was moved in steps of ≈7 cm by steps from the cell bottom upwards: for 4–5 cm the electrolyte temperature varied by a few hundredths of a degree centigrade, whereas it decreased by 0.15–0.2°C as the probe was moved further towards the surface. In a later test, the cell was equipped with a second Pt100 placed nearer to the heater (≈1.5 cm), but the temperature readings were only slightly higher (0.1–0.2°C) than those of the former. Therefore most places in the electrolyte, provided that they do not lie too near to either the heater or the electrolyte surface, are isothermal within 0.1–0.2°C.

The typical heating power necessary to maintain the electrolyte at 95°C in the various experiments was in the range 2.75–2.90 W. This result can be considered satisfactory: although cell and equipment were the same, we in fact changed from run to run either the volume of the electrolyte or the water source used in the refrigerating column (see above, tap water was at 15–16°C, whereas deep water was at 18°C). When a light water electrolyte was used, the power necessary to maintain it at 95.0°C was >3 W, in good agreement with our calorimetry predictions: light water boils 1°C lower than heavy water and, consequently, at 95°C the heat loss by evaporation is larger for H_2O than D_2O. In this latter aspect the barometric pressure may have some effect on the temperature of the electrolyte for a given input power. The influence of changes in the barometric pressure was not investigated: however, since the experiments were prolonged during varying seasons the possible effects are expected to cancel each other.

When bath and electrolyte were isothermal, calorimetry could be performed by two procedures:

(1) Non-isothermal, whereby the cell constant (°C W^{-1}) was determined by supplying an incremental power step to the heater and then recording the temperature response of the cell. Since the cell constant decreases with temperature owing to increased D_2O evaporation, more than one constant was determined at power steps of different amplitudes. Fig. 2 shows the typical calibration curve obtained with a power step of 0.92 W from the cell charged with 90 ml of D_2O + 0.6M K_2CO_3. The cell constant here was 2.2°C W^{-1}.

(2) The latter procedure kept isothermal conditions steady. Evaluation of the cell constant was not strictly necessary: when a thermal event occurred in the cell the power at the heater was adjusted to balance this event, the extent of which was thus immediately determined.

During the electrolytic runs, both procedures were adopted. In the initial stage (one or more hours), free temperature evolution above (or below) 95.0°C was generally allowed: the temperature increment was then converted into power by previous calibration. In subsequent stages, the heater power was generally reduced to balance the additional heat in the electrolyte.

It must be noted that, when electrolysis was underway, the power measurements performed by either of the two procedures did not give the whole (real) incremental power. Electrolytic splitting of D_2O produces gaseous products which, in the adopted calorimetry, induce further evaporation with further heat loss. To account for this additional loss, the thermal characteristics of the system were evaluated (both in the blanks and during electrolysis) while N_2 flow-rate was varied. For instance, when the electrolyte was at 95.0°C, N_2 flow-rate was increased by steps and for each step the incremental power given to the heater to maintain the electrolyte at 95.0°C was determined. Likewise, the cell constants determined in the absence of electrolysis for more than one gas flow-rate were compared with those obtained when electrolysis was running at a given current intensity. Thus, the heat loss measured, for instance, with an incremental flow-rate of 1.5 ml min^{-1}, which corresponds to the gas evolving from a current of 0.15 A, was in the range 0.20–0.23 W. Such additional power was used to correct the direct calorimetric measurement.

2.3.3. Electrolytic runs

Electrolysis was carried out by applying a dc current between cathode and anode. The maximum current intensity used was 0.275 A; the galvanostat assured current stability at 1%, and oscillations or alternating components were either absent or totally negligible.

The total power entering the cell by electrolysis was thus:

$$P_E \text{ (in W)} = I \text{ (in A)} \times E \text{ (in V)} \quad (1)$$

where I is dc current intensity and E is the difference of potential between the electrodes.

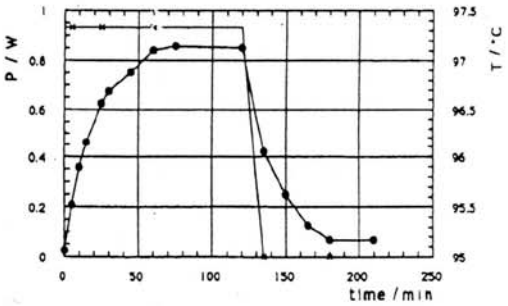

Fig. 2. Typical calibration curve. (×) Power step by the heater (left ordinate); (●) temperature response by the calorimeter (right ordinate).

The Joule power accomplishing electrolysis is given by:

$$P_J = I(E - 1.52) \quad (2)$$

where 1.52 was used as the thermoneutral potential necessary for D_2O splitting.

When working in non-isothermal conditions the heat input in the cell (in the absence of anomalous heat excess) was:

$$P_{input} = P_R^\circ + P_J(t) \quad (3a)$$

where P_R° is the power supplied ab initio by the heater to maintain the electrolyte at 95.0°C and $P_J(t)$ accounts for the possible variation in Joule heating with electrolysis time.

Excess heating power, if any, is thus determined as:

$$P_{ex(m)}(t) = \Delta T/k - P_J(t) \quad (3b)$$

where k is the cell constant in °C W^{-1} and ΔT is the temperature increase.

When working in isothermal conditions, the excess power was given at any time by:

$$P_{ex(m)}(t) = P_R^\circ - P_R(t) - P_J(t) \quad (4a)$$

where $P_R(t)$ is the power adjusted to maintain the electrolyte at 95.0°C.

Apparent excess power ($P_{ex(m)}$) was measured, using either Eq. (3b) (and calibration) or Eq. (4a) (straight away), while real power ($P_{ex(c)}$) is obtained as:

$$P_{ex(c)} = P_{ex(m)} + \Delta P_{gas} \quad (4b)$$

where ΔP_{gas} is the power correction due to the electrolytic gas.

2.3.4. Accuracy

As already mentioned, the oil bath was thermostated at ±0.01°C, while cell temperature readings were made of ±1 μA sensitivity which, depending on the sensor used, corresponded to 0.009 and 0.012°C respectively; once temperature had been converted into power (by calibration), the latter was measured with typical sensitivity of 4 or 6 mW.

However, considering possible cell temperature fluctuations due to either room temperature fluctuations or changes in the solution volume[1], the temperature of the electrolyte was actually measured with an accuracy of ±10 μA and consequently σ was ±40 or ±60 mW.

When converting $P_{ex(m)}$ into $P_{ex(c)}$, σ had to be increased by the error linked to the evaluation of heat loss caused by the electrolytic gas.

For this calorimetric system the claimed accuracy was achieved provided gas flow-rate was carefully controlled. Manually operated valves (Regulators HBS-HBSI, L'Air Liquide, Montigny) generally allow a very good control of gas flow-rate for relatively short periods (≤1 h): afterwards the gas flow tends to either increase or decrease (occasionally, ±30–40% in 10–12 h). Therefore we were checking and/or adjusting the bubbles to 62 ± 1 min^{-1} at any 15 min: this manual intervention was possible for 12 h during the day but not at night. In reporting the results below it was assumed that the thermal conditions at night were those obtained by averaging the last measurement in the evening with the first one of the following morning, once we had checked and/or adjusted the bubble flow.

[1] D_2O refilling was done in batches, not continuously.

3. Results

3.1. Experimental design

Six experiments, numbered progressively from 1 to 6, were performed: each experiment lasted from ≈1 to ≈3 weeks. The electrolyte, D_2O + 0.6 M K_2CO_3 was always the same, but exp. 6 was carried out in the light water analogue. One or maximum 2 ml of D_2O + 0.5 M thiourea were generally added to the electrolyte during the second or a successive refilling.

The main difference from run to run concerned the design of the cathode. Thus, in exps 1–3 the thickness of the Pd strip cathode was the same, but the area was different. Since the relaxation time of deuterium within a Pd sample depends on thickness, when the same current density was applied these electrodes were expected both to achieve the same D/Pd atom ratio and to generate excess enthalpy (if any) after the same electrolysis time: therefore, how the magnitude of the phenomenon depended on the size of the Pd specimen could be examined.

The cathode used in exp. 4 had the same area as that used in exp. 1, but was 2.5 times thicker. By comparing the results (if any) obtained in the two experiments, surface from bulk effects could be discriminated.

In exp. 5, the cathode was a rod, so that its surface/mass ratio was further decreased with respect to exp. 4.

3.2. Experiments 1–3

3.2.1. Exp. 1

Characteristics of the Pd strip cathode: dimensions, (1.3 × 2.5 × 0.02) cm^3; weight, 0.78 g.

Electrolysis was initiated with 0.023 A cm^{-2} (I = 0.150 A) applied: the calorimetric data correspondingly measured during the first 100 min of electrolysis, given as excess power $P_{ex(m)}$ (full squares), are compared in Fig. 3 with Joule power P_J fed by the current (small crosses).

The system was seen initially to absorb but not to produce power: in other words, during the first 10–15

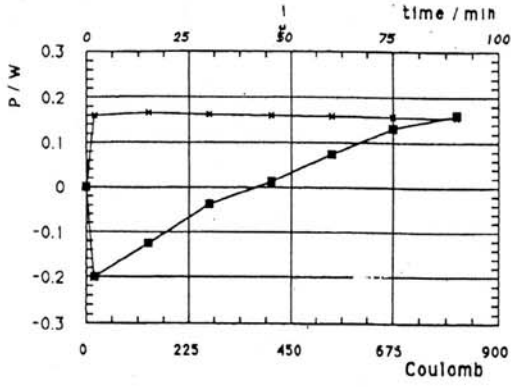

Fig. 3. Calorimetry of the first 100 min of exp. 1. (■) $P_{ex(m)}$ (measured excess power); (×) P_J (Joule power input).

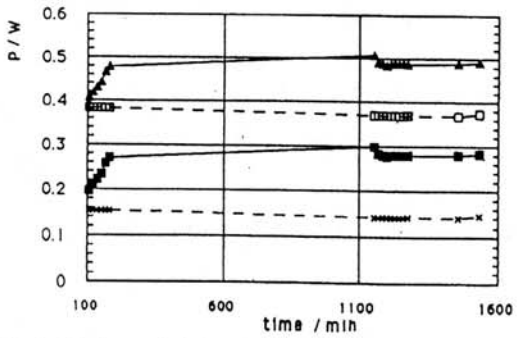

Fig. 4. Calorimetry of the first electrolysis day of exp. 1. (■) $P_{ex(m)}$; (▲) $P_{ex(c)}$ (corrected excess power); (×) P_J; (□) P_E (overall power supplied by the galvanostat).

min (100–150 Coulomb) the Joule heat input was not enough to balance the heat loss caused by the gas produced by electrolysis. But this trend was soon reversed, so that after 45 min (≈400 Coulomb) thermal balance was achieved ($P_{ex(m)} = 0.00$ W), and after 90 min an additional exothermic process became comparable to the Joule power input ($P_{ex(m)}/P_J(\%) \approx 100$).

Two observations may therefore be made regarding Fig. 3.

The first concerns the correlation between excess power and concentration of deuterium in the Pd sample. To achieve a D/Pd ratio in the range 0.8–0.85, which predictably is the maximum obtainable loading at 95°C, much more than 550–600 Coulomb had to be applied, since the efficiency of the electrolysis was very probably < 100%. However, Fig. 3 shows that the measurable excess power was obtained with defective stoichiometries (D/Pd ≤ 0.5–0.6 as averaged on the entire sample), but some heat evolution had probably occurred since the β-deuteride phase nucleated.

The second observation is that the excess power measured in this initial stage of the experiment is only partially accounted for by the enthalpy of PdD_x formation (37 kJ mol^{-1} [13]). In the adopted conditions, with $I = 0.15$ A and electrode weight $= 7.3 \times 10^{-3}$ mol, and assuming 100% efficiency for PdD_x formation (which is again an unrealistic figure), the expected thermal power was ≤ 0.03 W distributed for 1–1.5 h.

Fig. 4 shows the subsequent time evolution (while I was maintained at 0.150 A) of the thermal phenomenon. Other than $P_{ex(m)}$ (full squares) and P_J (small crosses), two other parameters are plotted here: $P_{ex(c)}$ (triangles) and P_E (empty squares). Thus, about 1 day after the experiment started, $P_{ex(m)}$ more than doubled P_J, and $P_{ex(c)}$, which represents the real excess power output, was larger than P_E which comprises the power necessary for D_2O splitting. Fig. 4 also shows that any increase in $P_{ex(m)}$ or $P_{ex(c)}$ was paralleled by a slight continuous decrease in P_J or P_E (the phenomenon is more evident in the subsequent experiments: exp. 3, Table 3, and exp. 4, Fig. 10): this point had already been noted by Fleischmann et al. [3,11].

During the next few days, the electrolysis current was either increased or decreased, and for each current the calorimetric response, plotted in Fig. 5 (as $P_{ex(c)}$) as a function of current density, was recorded when steady-state conditions had been attained. At the highest cur-

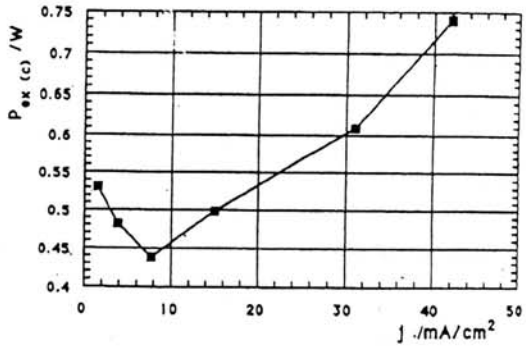

Fig. 5. $P_{ex(c)}$ in exp. 1 obtained for different current densities applied.

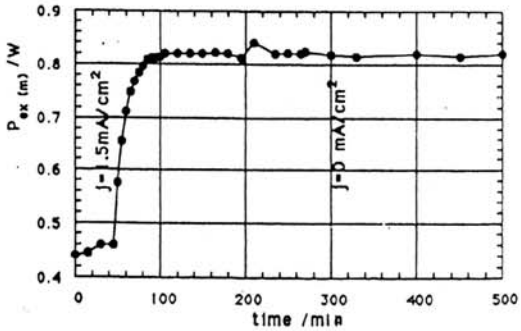

Fig. 6. $P_{ex(m)}$ obtained in exp. 1 when the cell was led to o.c. conditions.

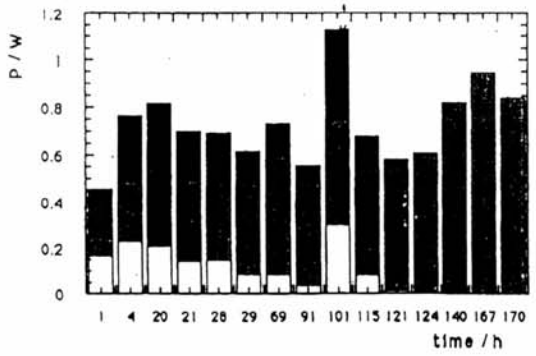

Fig. 7. Histograms accounting for the calorimetry of exp 1. White histogram, P_j; dotted histogram, P_m (measured power output); black histogram, P_c (corrected power output).

rent the largest heat evolution was predictably observed, but as j fell below 10 mA cm^{-2}, the excess power generation reverted its previous trend to increase again. This effect was magnified by interrupting the current applied (1.5 mA cm^{-2}) as shown in Fig. 6: the system taken to o.c. generated the greatest amount of power ever observed during this experiment. The phenomenon continued for more than 2 days until the experiment was deliberately stopped by turning off the heater and thermostatic bath: the electrode withdrawn from the cell at room temperature gave no sign of further heat emission.

The histograms in Fig. 7 explain the calorimetric history of the experiment: the white histogram is P_j input; the dotted one represents actually measured output power, P_m; and the black one is output power corrected by the electrolytic gas effect, P_c. By subtracting from P_m or P_c, the corresponding P_j, $P_{ex(m)}$ or $P_{ex(c)}$ are immediately obtained.

The remarkable point revealed by Fig. 7 is that the Joule energy input is many time lower than the energy output.

Table 1 lists the electrolysis conditions and calorimetric results: the last column clearly highlights the relative magnitude of the thermal phenomenon.

3.2.2. Exp. 2

Pd strip cathode characteristics: dimensions, (1.1 × 1.3 × 0.02) cm^3; weight, 0.3432 g.

Electrolysis was initiated at a current density of 0.023 A cm^{-2} (I = 0.065 A), which was maintained for about 18 h: during this period the features of exp. 1 (see Figs. 4 and 5) were substantially reproduced except for the magnitude of the anomalous heat effect, which was lower. After that, electrolysis periods of high/low current were alternated for some hours in o.c. conditions; and after about 5 days the excess power had increased to the steady values reported in Table 2. The last row indicates the excess heat produced when the electrolysis was finally interrupted. Comparing Tables 2 and 1, the intrinsic extent of the excess power is lower with the smaller electrode, but if the data are normalised to weight or area, the smaller sample shows higher specific efficiency. This type of performance is notably due to the electrolysis conditions adopted here (high/low current) which seem to be suitable to maximising the thermal phenomenon.

3.2.3. Exp. 3

Pd strip cathode characteristics: dimensions, (1.27 × 4.16 × 0.02) cm^3; weight, 1.226 g.

Electrolysis was always carried out at 0.023 A cm^{-2} (I = 0.243 A); since other current densities were not used, maximum heat generation was promoted by alternating electrolysis periods (two or more days) with long o.c. interruptions. This procedure also gave better knowledge of the 'after-effect', i.e. the heat output from the deuteride electrode in the absence of electrolysis.

Calorimetric data recorded during the first hour of electrolysis were similar to those reported in Figs. 3 and 4, except for the increased extent of the power excess. The subsequent evolution of the experiment is shown in the histograms in Fig. 8, which illustrate calorimetry from day 1 to day 21.

Points to be noted are: (1) heat generation (excess power output) under current flow initially increased and then reached stable values in about 4 days; (2) in contrast, the 'after-effect' steadily increased after each electrolysis period; (3) power oscillations in o.c. were mainly due to deuterium immissions into the cell (see Section 3.5); (4) the time decay of the 'after-effect' was very slow, as predicted. The operating conditions and the excess power actually measured in the several stages of the experiments are reported in Table 3. A quantitative energy balance could easily be obtained from the power input and the output integrated over 21 days, as shown in Table 3. Any comment seems to be superfluous.

3.3. Exp. 4

Pd strip cathode characteristics: dimensions, (1.3 × 2.5 × 0.05) cm^3; weight, 1.934 g.

Fig. 9 shows the calorimetric response during the first 3 h of electrolysis, performed at the same current density (0.023 A cm^{-2}) and consequently the same intensity (0.150 A) as in exp. 1.

Note the excess power, correlated with the D/Pd ratio, achieved by this electrode in the theoretical (unrealistic) hypothesis of deuterium insertion into Pd at 100% current efficiency. After an initial power absorption, the system achieved its original thermal balancing ($P_{ex(m)}$ = 0.00 W) in about 35 min with the passage of 315 Coulomb (D/Pd = 0.18). Some excess power could

Table 1
Conditions and calorimetric data of exp. 1

I /mA	j /mA cm^{-2}	P_E /W	P_J /W	$P_{ex(m)}$ /W	$P_{ex(c)}$ /W	$P_{ex(c)}/P_J$ /%
275	42.3	0.725	0.307	0.36 ± 0.04	0.74 ± 0.12	241
200	31	0.513	0.209	0.33 ± 0.04	0.61 ± 0.10	292
150	23	0.393	0.165	0.28 ± 0.04	0.49 ± 0.08	297
50	7.7	0.110	0.035	0.37 ± 0.04	0.44 ± 0.05	1257
25	3.8	0.051	0.013	0.45 ± 0.04	0.48 ± 0.05	3692
10	1.5	0.019	0.004	0.53 ± 0.04	0.53 ± 0.04	13 250
0	0	0.000	0.000	0.82 ± 0.04	0.82 ± 0.04	

Table 2
Conditions and calorimetric data of exp. 2

I /mA	j /mA cm^{-2}	P_E /W	P_J /W	$P_{ex(m)}$ /W	$P_{ex(c)}$ /W	$P_{ex(c)}/P_J$ /%
260	90	0.759	0.363	0.06 ± 0.06	0.46 ± 0.14	127
130	45	0.340	0.143	0.25 ± 0.06	0.45 ± 0.11	315
65	23	0.137	0.039	0.42 ± 0.06	0.52 ± 0.09	1333
15	5.2	0.026	0.003	0.48 ± 0.06	0.50 ± 0.07	16 667
10	3.5	0.018	0.003	0.36 ± 0.06	0.37 ± 0.07	12 333
5	1.7	0.008	0.001	0.31 ± 0.06	0.32 ± 0.07	32 000
0	0		0.000	0.63 ± 0.06	0.63 ± 0.06	

be measured after 50 min with 450 Coulomb (D/Pd = 0.25), and was nearly equal to the Joule power input in about 100 min with 900 Coulomb (D/Pd = 0.51). Eventually, when a D/Pd ratio of 0.85 might theoretically have been reached (165 min, near 1500 Coulomb) the extent of the excess power was nearly twice the P_J input. Therefore, comparing Figs. 9 and 3, we can see that similar P_{ex} were measured in the two experiments after the passage of the same amount of current. The obvious conclusion is that the excess heat correlates not with the (average) D/Pd ratio in the sample but with the amount of nucleated (active) β-deuteride phase. Fig. 10 shows calorimetric results during the subsequent 4 days. After about 24 h, $P_{ex(m)}$ was of the same extent as the overall power (P_E) entering the cell; in 3 days it even doubled P_E input. During day 5, higher and lower

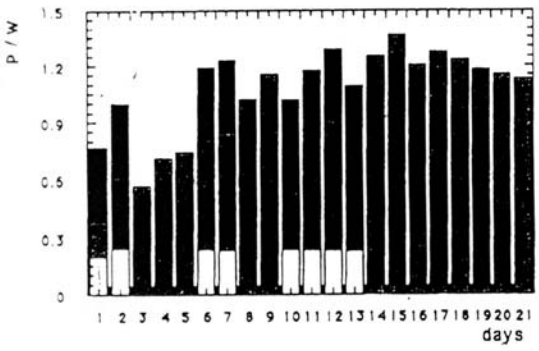

Fig. 8. Histograms accounting for the calorimetry of exp. 3. White histogram, P_j; dotted histogram, P_m; black histogram, P_c.

current densities were applied and thereafter the cell was taken to o.c. conditions: data are reported in Table 4. The excess power values here are larger than those of Table 1 when high current densities were applied: lower excess power was measured at low currents and in o.c. The explanation may be the following: more or less prolonged electrochemical activation is required to maximize the thermal phenomenon: the time-scales of exp. 1 and exp. 4 were the same, sufficient for the electrode in exp. 1, but not enough for the thicker electrode in exp. 4.

3.4. Exp. 5

Pd rod cathode characteristics: $\emptyset = 0.4$ cm; $l = 1.45$ cm; weight, 2.187 g.

Fig. 11 shows calorimetric data for the first 3.5 days of this experiment, steadily carried out with 0.024 A cm^{-2} ($I = 0.050$ A) of electrolysis current. Fig. 11 substantially shows that: (1) initially, the period of apparent power absorption was longer than in the preceding experiments; (2) $P_{ex(m)}$ reached the value of P_J after more than 8 h; (3) $P_{ex(m)}$ increased further for more than 1 day and then dropped suddenly (the fall coincided with the first (cold) D_2O refilling; (4) $P_{ex(m)}$ eventually rose again, but after a relatively long period. During the subsequent week, the trend shown in Fig. 11 did not change (D_2O refillings were again very critical): the data for this period are summarized in Table 5.

Fig. 12 shows the time evolution of the 'after-effect' measured from the moment when the cell was taken to o.c.: the heat output remained more or less constant for

Table 3
Conditions and calorimetric data of exp. 3[c]

Days	I /mA	j /mA cm^{-2}	P_g /W	P_j /W	$P_{ex(m)}$ /W[a]	$P_{ex(c)}$ /W	E_j /MJ	E_g /MJ	$E_{ex(m)}$ /MJ	$E_{ex(c)}$ /MJ
1	243	23	0.566	0.201	0.185	0.57 ± 0.13	0.038	0.102	0.048	0.114
2	243	23	0.615	0.245	0.372	0.75 ± 0.13				
3	0	0	0	0	0.566	0.57 ± 0.06	0	0	0.174	0.174
4	0	0	0	0	0.710	0.71 ± 0.06				
5	0	0	0	0	0.743	0.74 ± 0.06				
6	243	23	0.607	0.240	0.570	0.95 ± 0.13	0.041	0.105	0.102	0.168
7	243	23	0.605	0.235	0.610	0.99 ± 0.13				
8	0	0	0	0	1.020	1.02 ± 0.06	0	0	0.188	0.188
9	0	0	0	0	1.150	1.15 ± 0.06				
10	243	23	0.615	0.238	0.400	0.78 ± 0.13	0.081	0.209	0.182	0.310
11	243	23	0.608	0.236	0.557	0.94 ± 0.13				
12	243	23	0.600	0.235	0.670	1.05 ± 0.13				
13	243	23	0.600	0.232	0.480	0.87 ± 0.13				
14	0	0	0	0	1.25	1.25 ± 0.06	0	0	0.844	0.844
15	0	0	0	0	1.36	1.36 ± 0.06				
16	0	0	0	0	1.20	1.20 ± 0.06				
17	0	0	0	0	1.27	1.27 ± 0.06				
18	0	0	0	0	1.23	1.23 ± 0.06				
19	0	0	0	0	1.18	1.18 ± 0.06				
20	0	0	0	0	1.15	1.15 ± 0.06				
21	0	0	0	0	1.13	1.13 ± 0.06				

Total energy balance: $E_{input} = 0.42$ MJ; $E_{net\ produced} = 1.8 \pm 0.16$ MJ.
[a] $\sigma = 0.06$ W.

several hours. It fell to about one-third when 2.5 ml of cold D_2O was added (arrow 1); and then vanished (arrow 2). At the point indicated by arrow 2, both the thermostatic bath and the heater had been turned off to take the system to room temperature; on restoring the original heating conditions, the electrolyte equilibrated with the thermostatic bath at 95°C without any sign of additional heat sources present in the system.

The excess heat generation was lower than expected and was greatly affected by small temperature perturbations (1–3°C): (1) the correlation between Pd electrode mass and heat output was disregarded here (see above); (2) although the thermal phenomenon was generally reduced by the addition of cold water (the power fluctuations in Figs. 4 and 10 are related to D_2O refillings), the original heat output was soon re-established in exps. 1–4. The present behaviour may therefore be ascribed to the shape of the electrode (see below).

3.5. Interaction of deuteride electrodes with gaseous hydrogen

The influence of gaseous hydrogen on the 'after-effect' was investigated in exps. 1, 3 and 4, and was easily performed by exchanging the N_2 line for the D_2 (or H_2)

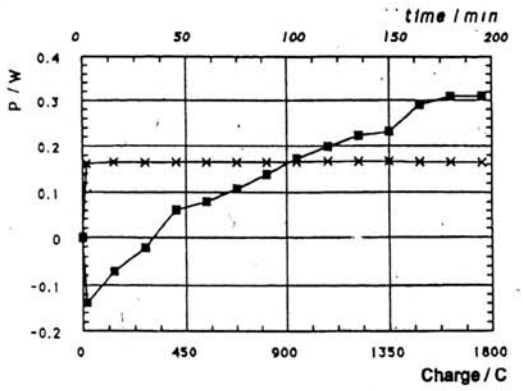

Fig. 9. Calorimetry of the first 200 min of exp. 4. (■) $P_{ex(m)}$; (×) P_j.

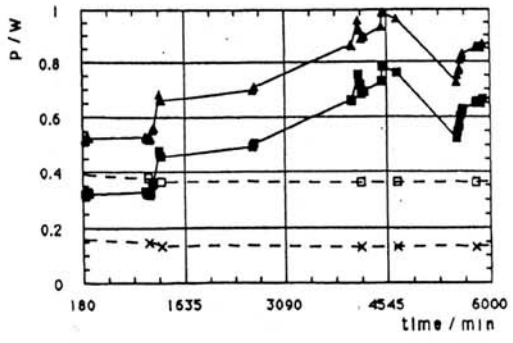

Fig. 10. Calorimetry of the first 4 days of exp. 4. (■) $P_{ex(m)}$; (▲) $P_{ex(c)}$; (×) P_j; (□) P_g.

Table 4
Conditions and calorimetric data of exp. 4

I /mA	J /mA cm^{-2}	P_E /W	P_J /W	$P_{ex(m)}$ /W	$P_{ex(c)}$ /W	$P_{ex(c)}/P_J$ /%
250	38.5	0.638	0.258	0.61 ± 0.04	0.94 ± 0.11	364
150	23	0.365	0.137	0.67 ± 0.04	0.87 ± 0.08	635
100	15.4	0.239	0.087	0.66 ± 0.04	0.79 ± 0.07	908
50	7.7	0.099	0.024	0.58 ± 0.04	0.65 ± 0.05	2708
25	3.8	0.048	0.010	0.43 ± 0.04	0.46 ± 0.05	4600
10	1.5	0.017	0.002	0.36 ± 0.04	0.37 ± 0.04	18 500
0	0	0.000	0.000	0.53 ± 0.04	0.53 ± 0.04	

line (at the same flow-rate) and then following the o.c. interaction of the PdD_x electrode with the hydrogen dissolved in the electrolyte by calorimetry.

Fig. 13 illustrates the results obtained in exp. 1: the arrows indicate the time at which either D_2 entered the system or N_2 flow was re-established. The heat output is seen to increase significantly, although with some delay after D_2 immission; this induction probably correlates with the saturation time of the electrolyte and the consequent equilibration of PdD_x with D_2. Some D_2 was in fact adsorbed, as the potential difference between the electrodes was later seen to reach a value larger than the initial one (some tens of mV). When N_2 was substituted for D_2, $P_{ex(m)}$ increased further before slowly decreasing to the original 'after-effect': the cathode/anode o.c. potential difference also decreased slightly to about the original value.

Fig. 14 shows the results of exp. 3, in which light hydrogen was the gas initially used. Although no apparent effect was measured, a $P_{ex(m)}$ increment occurred when N_2 replaced H_2. The effects obtained with later D_2 immission/outgassing were qualitatively and quantitatively similar to those shown in Fig. 13.

Fig. 15 gives the results of exp. 4. The effects, qualitatively similar to those of Figs. 13 and 14, were greater. $P_{ex(m)}$ definitely increased after the immission of light hydrogen, and the increment caused by D_2 was more than double that with previous Pd electrodes.

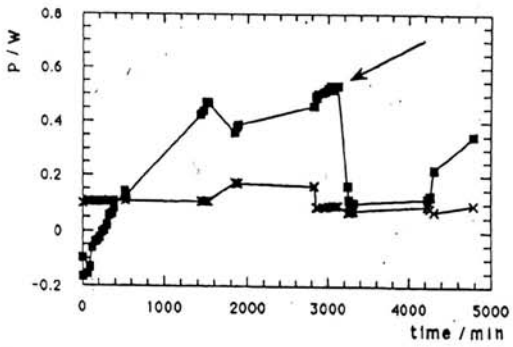

Fig. 11. Calorimetry of the first 3.5 days of exp. 5. (■) $P_{ex(m)}$; (×) P_J. The arrow indicates a first D_2O refilling.

3.6. Exp. 6

Pd strip cathode characteristics: dimension, (1.1 × 4.3 × 0.02) cm^3; weight, 1.112 g.

To maximise the heat effects which might originate in light water, the cathode was like that used in exp. 3, in which the largest heat output in D_2O had been tested; the same electrolysis procedure was used on alternating days with 0.023 A cm^{-2} (I = 0.218 A) steadily applied on days in o.c. conditions. The calorimetry of the first 5 h is shown in Fig. 16: after a short initial power drop, $P_{ex(m)}$ increased sharply for about 1 h and then dropped. During the subsequent hour $P_{ex(m)}$ again sporadically reached the value of P_J but was mostly within the measurement error.

The initial rise in $P_{ex(m)}$ may partly be explained by the enthalpy of PdH_x formation, but most of it was probably due to a different source: even when $P_{ex(m)}$ was within the error, the real excess power output, $P_{ex(c)}$ was some 10 mW above measurement error.

Fig. 17 illustrates the calorimetry of the whole experiment. The power output (dotted histogram) measured during electrolysis was the same as the P_J input (white histogram) or less: in other words, $P_{ex(m)}$ was always either at σ level or negative. However, on making due allowance for the heat loss caused by the electrolytic gas, the power output (P_c, black histogram) was about 0.3 ± 0.1 W. That some anomalous heat was also generated in light water was indicated by the calorimetric data obtained in o.c. conditions: a steady heat output (≈ 0.20 ± 0.06 W) was measured which, although many times lower than the phenomenon measured in D_2O (cf. Fig. 8) cannot be neglected. The decay in the heat output in o.c. conditions was faster than in experiments performed with D_2O, and was paralleled by a decay in the o.c. potential (i.e. the potential of PdH_x referred to nickel (oxide)), which was faster than for the heavy water analogue, as shown in Fig. 18. Since PdH_x was expected to have higher thermodynamic stability than PdD_x [13], the behaviour revealed by Fig. 18 is rather surprising.

Table 5
Conditions and calorimetric data of exp. 5[?]

I /mA	j /mA cm^{-2}	P_e /W	P_J /W	$P_{ex(m)}$ /W	$P_{ex(c)}$ /W	$P_{ex(c)}/P_J$ /%
250	121	0.695	0.315	0.40 ± 0.06	0.78 ± 0.12	248
150	72	0.381	0.153	0.53 ± 0.06	0.74 ± 0.10	484
100	48	0.241	0.089	0.49 ± 0.06	0.63 ± 0.08	708
50	24	0.110	0.034	0.48 ± 0.06	0.55 ± 0.07	1618
15	7.2	0.029	0.006	0.54 ± 0.06	0.56 ± 0.06	9333
10	4.8	0.018	0.003	0.61 ± 0.06	0.62 ± 0.06	20 667
5	2.4	0.009	0.001	0.58 ± 0.06	0.59 ± 0.06	59 000
0	0	0.000	0.000	0.56 ± 0.06	0.56 ± 0.06	

4. Discussion

The major achievement of this work is to have devised a temperature range in which the generation of excess power is a totally reproducible phenomenon. In fact, only a reproducible phenomenon can be investigated successfully, due to its dependence on the experimental variables. Here, the dependence of electrolysis time, current density, cathode shape, o.c. conditions, and presence of hydrogen in the electrolyte highlighted some correlations which, although they do not explain the excess power generation, may help to rationalize the phenomenon. Attention will be focused on these correlations.

4.1. Influence of loading

When suitable cathode geometry was adopted, excess power was produced despite defective D/Pd ratios, very probably as soon as some 'activated' β-deuteride was nucleated. This does not mean that Pd β-deuteride as such is generating heat: it was seen that even the small

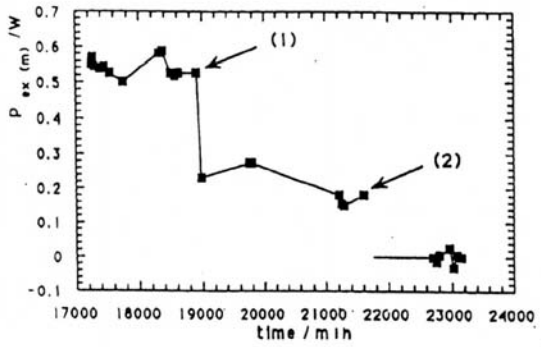

Fig. 12. $P_{ex(m)}$ at o.c. in exp. 5. Arrow (1) indicates a D_2O refilling; arrow (2) indicates the stage where the external heating was before being turned off and thereafter turned on.

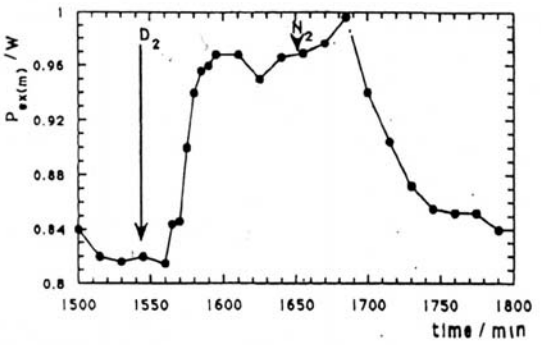

Fig. 13. Exp. 1: power output in o.c. conditions after successive immission/removal of D_2.

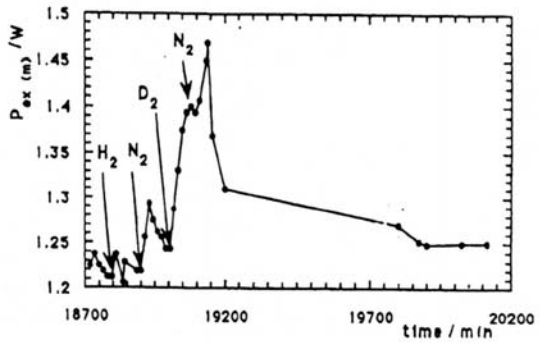

Fig. 14. Exp. 3: power output in o.c. conditions after successive immission/removal of either H_2 or D_2.

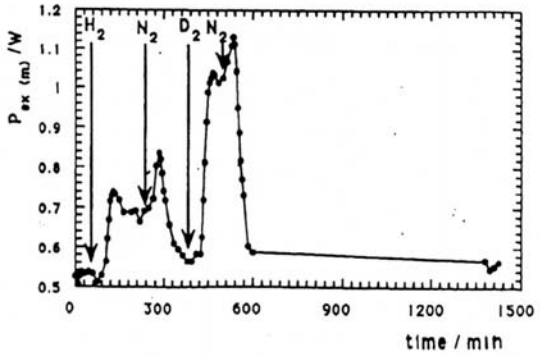

Fig. 15. Exp. 4: power output in o.c. conditions after successive immission/removal of either H_2 or D_2.

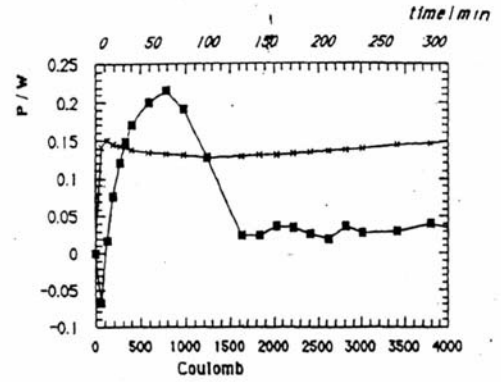

Fig. 16. Calorimetry of the first 300 min of exp. 6. (■) $P_{ex(m)}$; (×) P_j.

temperature decrease caused by D_2O refilling was enough to quench heat generation (cf. Figs. 11 and 12) but the chemical composition of β-deuteride (i.e. D/Pd ratio) definitely did not change. The term 'activated' is therefore used to indicate an energy state of β-deuteride (resonant phase, cooperative effects within coherence domains [14]) which may be triggered or otherwise by thermodynamic perturbations.

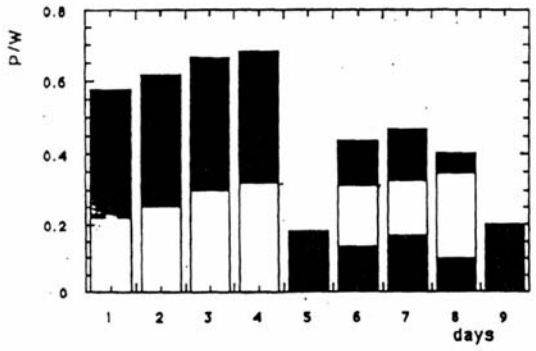

Fig. 17. Histograms accounting for calorimetry of exp. 6. White, P_j; dotted, P_m; black, P_e.

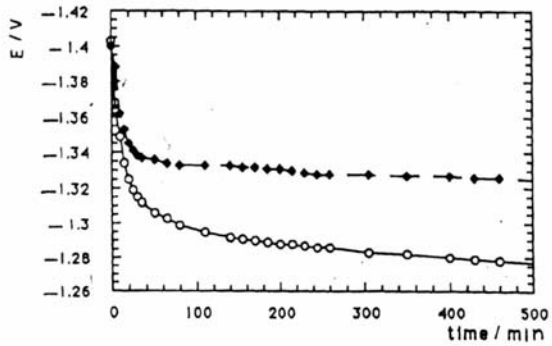

Fig. 18. O.c. potential decay for: (♦) D_2O–PdD_x system; (○) H_2O–PdH_x system.

4.2. Effect of applied current

The electrolysis current plays the basic role of nucleating the 'activated ' β-deuteride phase and leading it in time to maximum heat output. However once this situation has been achieved, the thermal phenomenon is clearly seen to depend on current density in a not unequivocal way (see, for instance, Fig. 5). This behaviour may be explained by assuming that heat is generated either by the bulk deuteride (the main effect) or by surface and near-surface sites. If the latter are activated through interaction with surface deuterium whose steady-state concentration increases with current, the parallel increase in excess power output is explained.

A different situation arises for the 'activated' bulk deuteride, whose thermodynamic potential is in (metastable) equilibrium with the Pd surface potential. Since this potential is determined by current density, the latter 'confines' and thus in someway stabilizes the 'deuteron plasma' within the Pd lattice. In this view, the greater the current density the more the deuteron is confined.

4.3. Cathode geometry

It has been shown that, within a homogeneous set of sample shapes (exps. 1–3, 4), heat generation is an extensive phenomenon which predictably increases with the size of the Pd samples. Poorer effects were obtained from a rod cathode (exp. 5) which had the largest mass but the smallest surface area: indeed, lower heat contribution was expected here from surface sites. However the exceedingly long electrolysis time required to establish excess power output (Fig. 11) as well as its critical sensitivity to small temperature decrements indicate that the rod shape is not the most suitable. Its low surface/mass ratio and consequent increased thickness makes electrolytic insertion less efficient and more time-consuming than for Pd sheets. Furthermore, current-induced surface potential perturbations, necessary for 'activating' the β-deuteride phase, are not easily driven into the bulk of the sample, owing to the strongly increased relaxation time of deuterium.

4.4. After-effect

Power output in the absence of any power input is the most remarkable instance of anomalous heat generation obtained in this work. This 'after-effect' may be explained by the comments made above for current: in o.c. conditions, 'confinement' by the current vanishes and the 'activated' β-deuteride phase finds itself in strong thermodynamic disequilibrium, so that the heat

generating process is further activated. What must instead be explained is the very slow decay of the phenomenon with time. In fact, based on thermodynamic considerations alone [13], in o.c. conditions, β-deuteride should decay, owing to its not negligible decomposition pressure at 95°C. This should be especially true under a N_2 flow (the actual conditions) continuously removing any D_2 freed by the sample. However, we have observed elsewhere [15] that, at 95°C the decomposition time-scale of deuterides of Pd 95%–Rh 5% alloy followed thermodynamic predictions for the gas/solid system, but it was some orders of magnitude slower in an electrolytic environment: a possible explanation for this behaviour was advanced in Ref. [15]. Now, considering that deuterides of Pd–Rh alloy are far more thermally unstable than Pd analogues, the stability assessed here is not surprising.

A second question concerns the nature of the process sustaining the power output in o.c. conditions for such long a time. Considering, for instance, the data of Table 3 (exp. 3), there is clearly no reasonable chemical explanation. However, if heat is generated by $D + D \rightarrow {}^4He + 24$ MeV fusion, steady power output of 1 W involves the consumption of $\approx 4.5 \times 10^{16}$ atoms day^{-1}: but the sample used in exp. 3, loaded to D/Pd = 0.8, as expected originally, contained $\approx 5.7 \times 10^{21}$ atoms, which means that heat output could indeed go on for a long time.

4.5. Effect of hydrogen

Some results reported in Section 3.5 (the influence of hydrogen on both electrolyte temperature and Pd electrode potential) were initially thought to indicate the occurrence of anomalous thermal effects from the interaction of gaseous hydrogen with PdD_x: however this view was challenged by the lake of correlation between size of the effect and area of the Pd sample, as expected for a surface phenomenon.

In a later stage of this investigation Figs. 13–15 were definitely shown to be a subtle artefact, at least with respect to the supposed hydrogen–PdD_x interaction: in fact the same thermal effects were observed by exchanging N_2 flow for D_2 flow into the Dewar cell deprived of the electrodes, containing only 0.6 M $K_2CO_3 + D_2O$ solution.

Therefore, from hydrogen bubbling into the electrolyte alone we observed that: the temperature increment caused by D_2 (with respect to N_2 at the same flow-rate) is largely above the error ($\geq 1.0°C \geq 10\sigma$); the effect is much larger for D_2 than for H_2 in agreement with Figs. 14 and 15; the effect progressively vanishes on diluting D_2 with other gases: for instance, the mixture 50% N_2 + 36% D_2 + 14% O_2 had approximately the thermal behaviour of pure N_2.

At first sight such observations are disconcerting, however anomalous effects are not necessarily involved and the matter could have a physical explanation: if at 95°C the various gases affect, in a different way, the evaporation of D_2O, the heat loss of the calorimeter and the temperature of the electrolyte are correspondingly varied.

Acknowledgements

One of the authors (M.B.) acknowledges the financial support of a fellowship by Edison s.p.a. Milano.

References

[1] M. Fleischmann, S. Pons, M. Hawkins, J. Electroanal. Chem. 261 (1989) 301.
[2] S.E. Jones, E.P. Palmer, J.B. Czirr, D.L. Decker, J.M. Thorne, S.F. Taylor, J. Rafelski, Nature 338 (1989) 737.
[3] M. Fleischmann, S. Pons, M.V. Anderson, L.J. Li, M. Hawkins, J. Electroanal. Chem. 287 (1990) 293.
[4] J.O. Bockris, G.H. Lin, N.G.C. Packam, Fusion Technol. 18 (1990) 11.
[5] M. Srinivasam, Curr. Sci. 60 (1991) 417.
[6] E. Storms, Fusion Technol. 20 (1991) 233.
[7] V.A. Tsarev, D.H. Wordledge, Fusion Technol. 20 (1991) 484.
[8] B.Y. Liaw, P.L. Tao, P. Turner, B.E. Liebert, J. Electroanal. Chem. 319 (1991) 161.
[9] A.B. Karabut, Ya.R. Kucherov, I.B. Savvatimova, Phys. Lett. A 170 (1992) 265.
[10] A.B. Karabut, Ya.R. Kucherov, I.B. Savvatimova, Proceedings of ICCF5, April 1995, p. 223.
[11] M. Fleischmann, S. Pons, Phys. Lett. A 176 (1993) 118.
[12] D. Morrison, Transaction of Fusion Technology, December 1994; pp. 48–55, vol. 26, number 4T (part 2) FUSTE8 (4) 1–540 (1994) ISSN: 0748–1896.
[13] F.A. Lewis, The Palladium Hydrogen System, Academic Press, London, 1967.
[14] G. Preparata, Fusion Technol. 20 (1991) 82.
[15] G. Mengoli, M. Fabrizio, C. Manduchi, G. Zannoni, J. Electroanal. Chem. 390 (1995) 135.